

COMPARISON OF k_T -FACTORIZATION APPROACH AND QCD PARTON MODEL FOR CHARM AND BEAUTY HADROPRODUCTION

M.G.Ryskin and A.G.Shuvaev
Petersburg Nuclear Physics Institute,
Gatchina, St.Petersburg 188350 Russia

Yu.M.Shabelski
The Abdus Salam International Centre
for Theoretical Physics, Trieste, Italy
and
Petersburg Nuclear Physics Institute,
Gatchina, St.Petersburg 188350 Russia¹

Abstract

We compare the numerical predictions for heavy quark production in high energy hadron collisions of the conventional QCD parton model and the k_T -factorization approach (semihard theory). The total production cross sections, one-particle rapidity and p_T distributions as well as two-particle correlations are considered. The difference in the predictions of the two approaches is not very large, while the shapes of the distributions are slightly different.

E-mail RYSKIN@THD.PNPI.SPB.RU

E-mail SHABELSK@THD.PNPI.SPB.RU

E-mail SHUVAEV@THD.PNPI.SPB.RU

¹Permanent address

1 Introduction

The investigation of heavy quark production in high energy hadron collisions is an important method for studying the quark-gluon structure of hadrons. Realistic estimates of the cross section of heavy quark production as well as their correlations are necessary in order to plan experiments on existing and future accelerators as well as in cosmic ray physics.

The description of hard interactions in hadron collisions within the framework of QCD is possible only with the help of some phenomenology, which reduces the hadron-hadron interaction to the parton-parton one via the formalism of the hadron structure functions. The cross sections of hard processes in hadron-hadron interactions can be written as the convolutions squared matrix elements of the sub-process calculated within the framework of QCD, with the parton distributions in the colliding hadrons.

The most popular and technically simplest approach is the so-called QCD collinear approximation, or parton model (PM). In this model all particles involved are assumed to be on mass shell, carrying only longitudinal momenta, and the cross section is averaged over two transverse polarizations of the incident gluons. The virtualities q^2 of the initial partons are taken into account only through their structure functions. The cross sections of QCD subprocess are calculated usually in the leading order (LO), as well as in the next to leading order (NLO) [1, 2, 3, 4, 5]. The transverse momenta of the incident partons are neglected in the QCD matrix elements. This is the direct analogy of the Weizsaecker-Williams approximation in QED. It allows to describe quite reasonably the experimental data on the total cross sections and one-particle distributions of produced heavy flavours, however it can not reproduce, say, the azimuthal correlations [6] of two heavy quarks, as well as the distributions of the total transverse momentum of heavy quarks pairs [7], which are determined by the transverse momenta of the incident partons.

There is an attempt to incorporate the transverse momenta of the incident partons by a random shift of these momenta (k_T kick) [7] according to certain exponential distributions. This allows to describe quantitatively the two-particle correlations [7], but it creates the problems in the simultaneous description of one-particle longitudinal and transverse momentum distributions [8].

Another possibility to incorporate the incident parton transverse momenta is referred to as k_T -factorization approach [9, 10, 11, 12, 13], or the theory of semihard interactions [14, 15, 16, 17, 18, 19]. Here the Feynman diagrams are calculated taking account of the virtualities and of all possible polarizations of the incident partons. In the small x domain there are no grounds to neglect the transverse momenta of the gluons, q_{1T} and q_{2T} , in comparison with the quark mass and transverse momenta, p_{iT} . Moreover, at very high energies and very high p_{iT} the main contribution to the cross sections comes from the region of $q_{1T} \sim p_{1T}$ or $q_{2T} \sim p_{1T}$. The QCD matrix elements of the sub-processes are rather complicated in such an approach. We have calculated them in the LO. On the other hand, the multiple emission of soft gluons is included here. That is why the question arises as to which approach is more constructive.

Most of the published papers on k_T -factorization have presented no numerical results or presented rather incomplete ones. Old sets of structure functions have been used, and, sometimes, the parton model results obtained with a particular set are compared with k_T -factorization results based on another set.

In our previous paper [20] we have presented a comparison of results obtained with the help of k_T -factorization and the parton model. The main goal of the paper [20] was to demonstrate the differences in the qualitative and numerical predictions coming from the matrix elements. To simplify the calculations and to avoid various additional dependences we had used gluon distribution which had only a reasonable qualitative behaviour and a fixed value of α_S .

The aim of this paper is to present a comparison between the results of the conventional parton model and the k_T -factorization approach for the quantities which are measured experimentally. For this reason we use the realistic gluon distribution GRV94 [21] compatible with the most recent data, see discussion in Ref. [22].

Below we shortly repeat the main formalism of the approaches used, discuss the values of the parameters and present the numerical results on charm and beauty production obtained in the LO (and qualitatively in NLO) parton model and in the k_T -factorization approach.

2 Conventional parton model approach

The conventional parton model expression for the calculation of heavy quark hadroproduction cross sections has the factorized form [23]:

$$\sigma(ab \rightarrow Q\bar{Q}) = \sum_{ij} \int dx_i dx_j G_{a/i}(x_i, \mu_F) G_{b/j}(x_j, \mu_F) \hat{\sigma}(ij \rightarrow Q\bar{Q}) , \quad (1)$$

where $G_{a/i}(x_i, \mu_F)$ and $G_{b/j}(x_j, \mu_F)$ are the structure functions of partons i and j in the colliding hadrons a and b , μ_F is the factorization scale (i.e. virtualities of incident partons) and $\hat{\sigma}(ij \rightarrow Q\bar{Q})$ is the cross section of the subprocess which is calculated in perturbative QCD. The latter cross section can be written as a sum of LO and NLO contributions,

$$\hat{\sigma}(ij \rightarrow Q\bar{Q}) = \frac{\alpha_s^2(\mu_R)}{m_Q^2} \left(f_{ij}^{(o)}(\rho) + 4\pi\alpha_s(\mu_R) \left[f_{ij}^{(1)}(\rho) + \bar{f}_{ij}^{(1)}(\rho) \ln(\mu^2/m_Q^2) \right] \right) , \quad (2)$$

where μ_R is the renormalization scale and $f_{ij}^{(o)}$ as well as $f_{ij}^{(1)}$ and $\bar{f}_{ij}^{(1)}$ depend only on the single variable

$$\rho = \frac{4m_Q^2}{\hat{s}} , \quad \hat{s} = x_i x_j s_{ab} . \quad (3)$$

(In the factor $\ln(\mu^2/m_Q^2)$ we assume $\mu_R = \mu_F$ following [1]. In the case of different values of μ_R and μ_F , which is preferable for the description of the experimental data [7], Eq. (2) becomes more complicated.)

The expression (1) corresponds to the process shown schematically in Fig. 1a. The main contribution to the cross section at small x is known to come from gluons, $i = j = g$.

Usually in the parton model the values

$$\mu_F = \mu_R = m_Q \quad (4)$$

are used for the total cross sections and

$$\mu_F = \mu_R = m_T = \sqrt{m_Q^2 + p_Q^2} \quad (5)$$

for the one-particle distributions [7]. However we calculate the total cross sections of heavy quark production as the integrals over their p_T distributions, i.e. with scales (5).

Both in the parton model and in the k_T -factorization approach we take

$$m_c = 1.4 \text{ GeV}, \quad m_b = 4.6 \text{ GeV} , \quad (6)$$

for the values of short-distance perturbative quark masses [24, 25].

Another principal problem of the parton model is the collinear approximation. The transverse momenta of the incident partons, q_{iT} and q_{jT} are assumed to be zero, and their virtualities are accounted for through the structure functions only; the cross section $\hat{\sigma}(ij \rightarrow Q\bar{Q})$ is assumed to be independent of these virtualities. Naturally, this approximation significantly simplifies the calculations.

The conventional NLO parton model approach with collinear approximation works quite reasonably for one-particle distributions and for the total cross sections; at the same time it is in serious disagreement with the data on heavy quark correlations (without k_T kick introduction [7]).

3 Heavy quark production in the k_T -factorization approach

In the k_T -factorization approach the transverse momenta of the incident gluons in the small- x region result from the $\alpha_s \ln k_T^2$ diffusion in the gluon evolution. The diffusion is described by the function $\varphi(x, q^2)$ giving the gluon distribution at a fixed fraction of the longitudinal momentum of the initial hadron, x , and of the gluon virtuality, q^2 . At very low x that is to leading $\log(1/x)$ accuracy, it is approximately determined [14] via the derivative of the usual structure function:

$$\varphi(x, q^2) = 4\sqrt{2}\pi^3 \frac{\partial[xG(x, q^2)]}{\partial q^2} . \quad (7)$$

Such a definition of $\varphi(x, q^2)$ enables to treat correctly the effects arising from the gluon virtualities.

Although generally φ is a function of three variables, x , q_T and q^2 , the transverse momentum dependence is comparatively weak since $q_T^2 \approx -q^2$ for small x in LLA in agreement with q^2 -dependences of structure function. Note that due to QCD scaling violation the value $\varphi(x, q^2)$ for the realistic structure functions increases more fast with decreasing of x . Therefore at smaller x , larger q_T becomes important in the numerical calculations.

The exact expression of the q_T gluon distribution can be obtained as a solution of the evolution equation which, contrary to the parton model case, is nonlinear due to interactions between the partons in the small x region. The calculations [26] of the q_T gluon distribution in leading order using the BFKL theory [27] result in differences from our $\varphi(x, q^2)$ function given by Eq. (7) by only about 10-15%.

Here we deal with the matrix element accounting for the gluon virtualities and polarizations. Since it is much more complicated than in the parton model we consider only the LO of the subprocess $gg \rightarrow Q\bar{Q}$ which gives the main contribution to the heavy quark production cross section at small x , see the diagrams in Fig. 2. The lower and upper ladder blocks present the two-dimensional gluon functions $\varphi(x_1, q_1^2)$ and $\varphi(x_2, q_2^2)$.

Strictly speaking, Eq. (7) may be justified in the leading $\log(1/x)$ limit only. To restore the unintegrated parton distribution $f_a(x, q_T, \mu)$ (i.e. the probability to find a parton a with transverse momentum q_t which initiates our hard process, with factorization scale μ) based on the conventional (integrated) parton density $a(x, \lambda^2)$ we have to consider the DGLAP evolution²

$$\frac{\partial a}{\partial \ln \lambda^2} = \frac{\alpha_s}{2\pi} \left[\int_x^{1-\Delta} P_{aa'}(z) a' \left(\frac{x}{z}, \lambda^2 \right) dz - a(x, \lambda^2) \sum_{a'} \int_0^{1-\Delta} P_{a'a}(z') dz' \right] \quad (8)$$

(here $a(x, \lambda^2)$ denotes $xg(x, \lambda^2)$ or $xq(x, \lambda^2)$ and $P_{aa'}(z)$ are the splitting functions).

The first term on the right-hand side of Eq. (8) describes the number of partons δ_a emitted in the interval $\lambda^2 < q_t^2 < \lambda^2 + \delta\lambda^2$, while the second (virtual) term reflects the fact that the parton a disappears after the splitting.

The second contribution may be resummed to give the survival probability T_a that the parton a with transverse momentum q_t remains untouched in the evolution up to the factorization scale

$$T_a(q_t, \mu) = \exp \left[- \int_{q_t^2}^{\mu^2} \frac{\alpha_s(p_t)}{2\pi} \frac{dp_t^2}{p_t^2} \sum_{a'} \int_0^{1-\Delta} P_{a'a}(z') dz' \right] \quad (9)$$

Thus the unintegrated distribution $f_a(x, q_t, \mu)$ reads

$$f_a(x, q_t, \mu) = \left[\frac{\alpha_s}{2\pi} \Theta(1 - \delta - x) \int_x^{1-\Delta} P_{aa'}(z) a' \left(\frac{x}{z}, q_t^2 \right) dz \right] T_a(q_t, \mu), \quad (10)$$

where the cut-off $\delta = q_t/\mu$ is used both in Eqs. (9) and (10) [28, 29].

²For the $g \rightarrow gg$ splitting we need to insert a factor z' in the last integral of Eq. (8) to account for the identity of the produced gluons.

In the leading $\log(1/x)$ (i.e. BFKL) limit the virtual DGLAP contribution is neglected. So $T_a = 1$ and one comes back to Eq. (7)

$$f_a^{BFKL}(x, q_t, \mu) = \frac{\partial a(x, \lambda^2)}{\partial \ln \lambda^2} \quad , \lambda^\epsilon = q_t \quad . \quad (11)$$

In the double log limit Eq. (10) can be written in the form

$$f_a^{DDT}(x, q_t, \mu) = \frac{\partial}{\partial \ln \lambda^2} \left[a(x, \lambda^2) T_a(\lambda, \mu) \right]_{\lambda=q_t} \quad , \quad (12)$$

which was firstly proposed by [30]. In this limit the derivative $\partial T_a / \partial \ln \lambda^2$ cancels the second term of the r.h.s. of Eq. (8) (see [29] for a more detailed discussion).

Finally, the probability $f_a(x, q_t, \mu)$ is related to the BFKL function $\varphi(x, q_t^2)$ by

$$\varphi(x, q^2) = 4\sqrt{2} \pi^3 f_a(x, q_t, \mu) \quad . \quad (13)$$

Note that due to a virtual DGLAP contribution the derivative $\partial a(x, \lambda^2) / \partial \lambda^2$ can be negative for not small enough x values. This shortcoming of Eq. (11) is overcome partly in the case of Eq. (12). Unfortunately the cut-off Δ used in a conventional DGLAP computation does not depend on the scale μ . To obtain an integrated parton distributions it is enough to put any small $\Delta \ll 1^3$.

On the other hand, in the survival probability Eq. (9) we have to use the true (within the leading log approximation) value $\Delta = q_t / \mu$. Thus for a rather large q_t (of the order of μ) and x even the DDT form Eq. (12) is not precise enough. Only the expression (10) with the same cut-off Δ in a real DGLAP contribution and in survival probability (9) provides the positivity of the unintegrated probability $f_a(x, q_t, \mu)$ in the whole interval $0 < x < 1$.

Of course, just by definition $f_a(x, q_t, \mu) = 0$ when the transverse momentum q_t becomes larger than the factorization scale μ .

In what follows we use the Sudakov decomposition for quark momenta $p_{1,2}$ through the momenta of colliding hadrons p_A and p_B ($p_A^2 = p_B^2 \simeq 0$) and the transverse momenta $p_{1,2T}$:

$$p_{1,2} = x_{1,2} p_B + y_{1,2} p_A + p_{1,2T} \quad . \quad (14)$$

The differential cross section of heavy quark hadroproduction has the following form:⁴

$$\frac{d\sigma_{pp}}{dy_1^* dy_2^* d^2 p_{1T} d^2 p_{2T}} = \frac{1}{(2\pi)^8} \frac{1}{(s)^2} \int d^2 q_{1T} d^2 q_{2T} \delta(q_{1T} + q_{2T} - p_{1T} - p_{2T})$$

³There is a cancellation between the real and virtual soft gluon DL contributions in the DGLAP equation, written for the integrated partons (including all $k_t \leq \mu$). The emission of a soft gluon with momentum fraction $(1-z) \rightarrow 0$ does not affect the x -distribution of parent partons. Thus the virtual and real contributions originated from $1/(1-z)$ singularity of the splitting function $P(z)$ cancel each other.

On the contrary, in the unintegrated case the emission of soft gluon (with $q'_t > k_t$) alters the transverse momentum of parent (t -channel) parton. Eq. (8) includes this effect through the derivative $\partial T(k_t^2, \mu^2) / \partial k_t^2$.

⁴We put the argument of α_S to be equal to gluon virtuality, which is very close to the BLM scheme[31]; (see also [17]).

$$\times \frac{\alpha_s(q_1^2)}{q_1^2} \frac{\alpha_s(q_2^2)}{q_2^2} \varphi(q_1^2, y) \varphi(q_2^2, x) |M_{QQ}|^2. \quad (15)$$

Here $s = 2p_A p_B$, $q_{1,2T}$ are the gluon transverse momenta and $y_{1,2}^*$ are the quark rapidities in the hadron-hadron c.m.s. frame,

$$\begin{aligned} x_1 &= \frac{m_{1T}}{\sqrt{s}} e^{-y_1^*}, & x_2 &= \frac{m_{2T}}{\sqrt{s}} e^{-y_2^*}, & x &= x_1 + x_2 \\ y_1 &= \frac{m_{1T}}{\sqrt{s}} e^{y_1^*}, & y_2 &= \frac{m_{2T}}{\sqrt{s}} e^{y_2^*}, & y &= y_1 + y_2 \\ m_{1,2T}^2 &= m_Q^2 + p_{1,2T}^2. \end{aligned} \quad (16)$$

$|M_{QQ}|^2$ is the square of the matrix element for the heavy quark pair hadroproduction.

In LLA kinematic

$$q_1 \simeq y p_A + q_{1T}, \quad q_2 \simeq x p_B + q_{2T}. \quad (17)$$

so

$$q_1^2 \simeq -q_{1T}^2, \quad q_2^2 \simeq -q_{2T}^2. \quad (18)$$

(The more accurate relations are $q_1^2 = -\frac{q_{1T}^2}{1-y}$, $q_2^2 = -\frac{q_{2T}^2}{1-x}$ but we are working in the kinematics where $x, y \sim 0$).

The matrix element M is calculated in the Born approximation of QCD (see details in [18, 20] without standard simplifications of the parton model.

4 Total cross sections and one-particle distributions

Eq. (15) enables us to calculate straightforwardly all distributions concerning one-particle or pair production. One-particle calculations as well as correlations between two produced heavy quarks can be easily obtained using, say, the VEGAS code [32].

However there exists a principal problem coming from the infrared region. Since the functions $\varphi(x, q_2^2)$ and $\varphi(y, q_1^2)$ are unknown at small values of q_2^2 and q_1^2 we use the direct consequence of Eq. (7) [33]

$$xG(x, q^2) = xG(x, Q_0^2) + \frac{1}{4\sqrt{2}\pi^3} \int_{Q_0^2}^{q^2} \varphi(x, q_1^2) dq_1^2. \quad (19)$$

and rewrite the integrals in the Eq. (15) as

$$\begin{aligned}
& \int d^2 q_{1T} d^2 q_{2T} \delta(q_{1T} + q_{2T} - p_{1T} - p_{2T}) \frac{\alpha_s(q_1^2)}{q_1^2} \frac{\alpha_s(q_2^2)}{q_2^2} \varphi(q_1^2, y) \varphi(q_2^2, x) |M_{QQ}|^2 = \\
& = (4\sqrt{2} \pi^3 \alpha_s(m_T^2))^2 x G(x, Q_0^2) y G(y, Q_0^2) T^2(Q_0^2, \mu^2) \left(\frac{|M_{QQ}|^2}{q_1^2 q_2^2} \right)_{q_{1,2} \rightarrow 0} + \quad (20) \\
& + 4\sqrt{2} \pi^3 \alpha_s(m_T^2) x G(x, Q_0^2) T(Q_0^2, \mu^2) \int_{Q_0^2}^{\infty} dq_{1T}^2 \delta(q_{1T} - p_{1T} - p_{2T}) \times \\
& \quad \times \frac{\alpha_s(q_1^2)}{q_1^2} \varphi(q_1^2, y) \left(\frac{|M_{QQ}|^2}{q_2^2} \right)_{q_2 \rightarrow 0} + \\
& + 4\sqrt{2} \pi^3 \alpha_s(m_T^2) y G(y, Q_0^2) T(Q_0^2, \mu^2) \int_{Q_0^2}^{\infty} dq_{2T}^2 \delta(q_{2T} - p_{1T} - p_{2T}) \times \\
& \quad \times \frac{\alpha_s(q_2^2)}{q_2^2} \varphi(q_2^2, x) \left(\frac{|M_{QQ}|^2}{q_1^2} \right)_{q_1 \rightarrow 0} + \\
& + \int_{Q_0^2}^{\infty} d^2 q_{1T} \int_{Q_0^2}^{\infty} d^2 q_{2T} \delta(q_{1T} + q_{2T} - p_{1T} - p_{2T}) \times \\
& \quad \times \frac{\alpha_s(q_1^2)}{q_1^2} \frac{\alpha_s(q_2^2)}{q_2^2} \varphi(q_1^2, y) \varphi(q_2^2, x) |M_{QQ}|^2,
\end{aligned}$$

where the unintegrated gluon distributions are taken from Eqs. (9) and (10).

The first contribution in Eq. (20), with averaging of the matrix element over the directions of the two-dimensional vectors q_{1T} and q_{2T} , is exactly the same as the conventional LO parton model expression, with QCD scales $\mu_R^2 = m_T^2$ and $\mu_F^2 = Q_0^2$ multiplied by the 'survival' probability $T^2(Q_0^2, \mu^2)$ not to have transverse momenta $q_{1,2,T} > Q_0$. The sum of the produced heavy quark momenta is exactly zero here.

The next three terms contain the corrections to the parton model related to the gluon polarizations, virtualities and transverse momenta in the matrix element. The relative contribution of the corrections strongly depends on the initial energy. If it is not high enough, the first term in Eq. (20) dominates, and all results coincide practically (after accounting for Eq. (19)) with the conventional LO parton model predictions. In the case of very high energy the opposite situation takes place, the first term in Eq. (20) can be considered as a small correction and our results differ from the conventional ones. It is necessary to note that the absolute as well as the relative values of all terms in Eq. (20) strongly depend on the T-factor inclusion (i.e., when we use Eq. (10) or Eq. (7)).

Before the numerical comparison it is necessary to note that the NLO parton model actually results only in a normalization factor in the case of one-particle distributions, the shapes of LO and LO+NLO distributions are almost the same, see [3, 4, 5, 34]. This means that we can calculate the K-factor

$$K = \frac{\sigma(LO) + \sigma(NLO)}{\sigma(LO)}, \quad (21)$$

say, from the results for the total production cross sections, and restrict ourselves only to LO calculations of p_T , or rapidity distributions multiplying them by the K-factors.

The numerical values of the K-factors depend [35] on the structure functions used, quark masses, QCD scales and initial energy, the dependence on the renormalization scale μ_R being especially important. This seems to be evident, because the LO contribution is proportional to α_s^2 , whereas the NLO contribution is proportional to α_s^3 . However the more important dependence at high energies, when small ρ values dominate, comes from the structure of Eq. (2). At $\rho \rightarrow 0$ the functions $f_{gg}^{(1)}$ and $\bar{f}_{gg}^{(1)}$ have constant limits [1], $f_{gg}^{(1)}(\rho \rightarrow 0) \approx 0.1$ and $\bar{f}_{gg}^{(1)}(\rho \rightarrow 0) \approx -0.04$, so due to Eq. (2) the K factor at high energies depends strongly on the ratio μ/m_Q .

First of all let us present the role of the T -factors, Eq. (9). In Fig. 3 we show their values which were calculated as the ratios of the values of the first term of Eq. (20) to the same values calculated with $T_a(q_{1t}, \mu) = 1$ for the cases of charm and beauty production at $\sqrt{s} = 14$ TeV and $\mu^2 = \hat{s}$ as functions of q_{1t} . The values of heavy quark transverse momenta were fixed at 20 GeV/c. In both cases the values of $T_a(q_{1t})$ are rather small at small q_{1t} and $T_a(q_{1t}) \rightarrow 1$ at $p_t \gg q_{1t}$.

Now let us compare the numerical results predicted by the parton model and by the k_T -factorization approach.

The energy dependences of the total cross sections of $c\bar{c}$ and $b\bar{b}$ pair production are presented in Fig. 4. As was mentioned, at comparatively small energies the first term in Eq. (20) dominates and the results of the k_T -factorization approach should be close to the LO parton model prediction. Actually the first results are even smaller due to the presence of the T -factor in Eq. (10). However the k_T -factorization approach predicts a stronger energy dependence than the LO parton model both for $c\bar{c}$ and $b\bar{b}$ production. This can be explained by additional contributions appearing at very high energies in the k_T -factorization approach, see [20]

The calculated values of one-particle p_T distributions, $d\sigma/dp_T$, in the k_T -factorization approach and in the LO parton model are presented in Fig. 5. In all cases the k_T -factorization predicts broader distributions. The average values of p_T of the produced heavy quarks are rather different in these two approaches, as one can see from Table 1.

Table 1 The average values of charm and beauty quark transverse momenta $\langle p_T \rangle$ (in GeV/c) in the k_T -factorization approach with $\mu^2 = \hat{s}$ and in the LO parton model.

	LO parton model		k_T -factorization	
\sqrt{s}	$c\bar{c}$	$b\bar{b}$	$c\bar{c}$	$b\bar{b}$
14 TeV	1.78	4.53	2.23	5.47
1.8 TeV	1.48	3.96	1.91	4.54

It seems to be very natural, because, contrary to the case of the LO parton model, a large p_T of one heavy quark can be compensated not only by the p_T of another heavy quark but also by the initial gluons (i.e. by hard gluon jet emission).

The rapidity distributions of produced heavy quarks presented in Fig. 6 show that the main part of the difference between the k_T -factorization approach and the LO parton model comes from the central region.

5 Two-particle correlations

We saw from the previous section that there is only a small difference in our results for the total cross sections and one-particle distributions obtained in the k_T -factorization and in the LO parton model. The predictions of the NLO parton model for these quantities differ from the LO parton model only by a normalization factor of 2-2.5 [3, 4, 5, 34]. So the difference between our predictions and the NLO parton model should be small.

The calculations of two-particle correlations in different approaches are more informative. The simplest quantity here is the distribution in the total transverse momentum of the produced heavy quark pair, p_{pair} . In LO, evidently, $p_{pair} = p_{1T} + p_{2T} = q_{1T} + q_{2T}$, and if $q_{1T} = q_{2T} = 0$, then $d\sigma/dp_{pair}$ is a δ -function of zero. So the p_{pair} distributions give direct information about the transverse momentum distribution of the incident partons.

It is clear that if $q_{iT} \ll p_{iT}$, then the distributions in p_{pair} should be narrower in comparison with the one-particle p_T distributions. In this case the Weizsaecker-Williams approximation should be valid and one can believe that the parton model reflects the real dynamics of the interaction. In the opposite case, $q_{iT} \sim p_{iT}$, the large transverse momentum of the produced heavy quark can be compensated not by the other quark, but by a high- p_T gluon. We have shown in our previous paper [20], that about 70-80% of the total cross section of high- p_T quark production at high energies originates from such processes, when the heavy quark propagator is close to the mass shell.

We calculate the values of $d\sigma/dp_{pair}$ for charm (a) and beauty (b) production in the k_T -factorization approach using the unintegrated gluon distribution Eqs. (9), (10) with scale values $\mu^2 = \hat{s}$ and $\mu^2 = \hat{s}/4$ (only for $\sqrt{s} = 14$ TeV). Our results for pair production at different initial energies are shown by solid curves in Fig. 7. For the comparison we

present by dashed curves the one-particle p_T -distributions taken from Fig. 5, obtained in the same k_T -factorization approach and with the same T -factor. As we put $Q_0^2 = 1 \text{ GeV}^2$ in Eq. (20), we can not distinguish between the initial gluons with q_T equal to, say, $0.1 \text{ GeV}/c$ and $0.9 \text{ GeV}/c$, so our first bin in the $d\sigma/dp_{pair}$ distribution has the width $2 \text{ GeV}/c$ which explains some irregular behaviour of the solid curves at small p_T . Naturally, all the solid and dashed curves are normalized equally at the same energy.

At comparatively small energies, $\sqrt{s} = 39 \text{ GeV}$ and even at $\sqrt{s} = 630 \text{ GeV}$ the distributions $d\sigma/dp_{pair}$ are narrower than the one-particle distributions $d\sigma/dp_T$. This means that the transverse momenta of the produced heavy quarks almost completely compensate each other. However the situation changes drastically with increasing of the initial energy. Starting from comparatively small p_T , the difference between the curves decreases with energy. At $\sqrt{s} = 14 \text{ TeV}$ the distributions are similar both in the cases of $c\bar{c}$ and $b\bar{b}$ production. This means that the production mechanism changes in the discussed energy region. At $\sqrt{s} = 14 \text{ TeV}$ the transverse momentum of the produced heavy quark is balanced more probably by one or several gluons (see also [20]), because the contribution with large virtuality in the quark propagator is more suppressed in comparison with the large virtuality in the gluon propagator.

The discussed behaviour depends on the value of the scale μ^2 in the T -factor, Eq. (9). The similar calculation at energy $\sqrt{s} = 14 \text{ TeV}$ with $\mu^2 = \hat{s}/4$ is shown in Fig. 7 for pair and single production by dash-dotted and dotted curves, respectively. Here the difference between these two curves is more significant and it becomes larger for lower energies.

The distributions of the produced heavy quark pair as a function of the rapidity gap $\Delta y = |y_Q - y_{\bar{Q}}|$ between quarks are presented in Figs. 8. Here the difference between the LO PM and the k_T -factorization predictions is not large again except for the region of very large Δy .

Another interesting correlation is the distribution in the azimuthal angle ϕ , which is defined as the opening angle between the two produced heavy quarks, projected onto the plane perpendicular to the beam and defined as the xy -plane. In the LO parton model the sum of the produced heavy quark momenta projected onto this plane is exactly zero, and the angle between them is always 180° . In the case of the NLO parton model the ϕ distribution is non-trivial [6], however the predicted distribution (without including the k_T kick) is narrower in comparison with the fixed target data [7].

The theoretical as well as experimental investigation of such distributions are very important to control our understanding of the considered processes. The problem is that in the case of one-particle inclusive distributions for heavy quark production in hadron collisions the sum of LO and NLO contributions of the parton model practically coincides [3, 4, 5, 34] with the LO contribution multiplied by K-factors. Therefore agreement with experimental data can be achieved for too small or too large NLO contribution by fitting one parameter, which can work as a normalization factor (say, the QCD scale). The deviation in azimuthal correlations from the trivial $\delta(\phi - \pi)$ distribution comes from NLO correction to PM. However the standard NLO contributions are not large enough for the description of the data and only the comparatively large intrinsic transverse

momentum of incoming partons (k_T -kick) allows to describe [7] the data.

Preliminary results for the azimuthal correlations in the k_T -factorization approach were considered in [19]. The main difference in the information coming from $d\sigma/dp_{pair}$ and $d\sigma/d\phi$ distributions is due to the comparatively slow heavy quark. It gives a negligibly small contribution to the $d\sigma/dp_{pair}$ in the first case, whereas in the second one each quark contributes to the distribution $d\sigma/d\phi$ practically independently of its momentum, so all corrections coming from quark confinement, hadronization and resonance decay can be important.

As was discussed above, the first contribution in Eq. (20) is the same as the conventional LO parton model in which the angle between the produced heavy quarks is always 180° . However the angle between two heavy hadrons can be slightly different from this value due to a hadronization processes. To take this into account we assume that in this first contribution the probability to find a hadron pair with azimuthal angle $180^\circ - \phi$ is determined by the expression

$$w_1(\phi) = \frac{p_h}{\sqrt{p_h^2 + p_t^2}}, \quad (22)$$

where $p_h = 0.2 \text{ GeV}/c$ is a transverse momentum in the azimuthal plane coming from the hadronization process. The other contributions of Eq. (20) result in a more or less broad ϕ distribution so we neglect their small modification due to hadronization.

The k_T -factorization approach predictions for the azimuthal correlation of heavy quarks produced in pp collisions are presented in Fig. 9 and one can see that they change drastically when the initial energy increases from fixed target to the collider region.

6 Conclusion

We have compared the conventional LO Parton Model (PM) and the k_T -factorization approach for heavy quark hadroproduction at collider energies using a realistic gluon (parton) distribution. Both the transverse momenta and rapidity distributions have been considered, as well as two-particle correlations, such as the distribution over the rapidity gap between two heavy quarks, their azimuthal correlations and distributions of the total transverse momentum of the produced heavy quark pair, p_{pair} .

It has been shown in [20] that the contribution of the domain with strong q_T ordering ($q_{1,2T} \ll m_T = \sqrt{m_Q^2 + p_T^2}$) coincides in k_T -factorization approach with the LO PM prediction. Besides this a very numerically large contribution appears at high energies in k_T -factorization approach in the region $q_{1,2T} \geq m_T$. It kinematically relates to the events where the transverse momentum of heavy quark Q is balanced not by the momentum of antiquark \bar{Q} but by the momentum of the nearest gluon.

This configuration is associated with the NLO (or even NNLO, if both $q_{1,2T} \geq m_T$) corrections in terms of the PM with fixed number of flavours, i.e. without the heavy

quarks in the evolution. Indeed, as was mentioned in [1], up to 80% of the whole NLO cross section originates from the events where the heavy quark transverse momentum is balanced by the nearest gluon jet. Thus the large "NLO" contribution, especially at large p_T , is explained by the fact that the virtuality of the t -channel (or u -channel) quark becomes small in the region $q_T \simeq p_T$ and the singularity of the quark propagator $1/(\hat{p} - \hat{q}) - m_Q$ in the "hard" QCD matrix element, $M(q_{1T}, q_{2T}, p_{1T}, p_{2T})$, reveals itself.

The double logarithmic Sudakov-type form factor T in the definition of unintegrated parton density (10) comprises an important part of the virtual loop NLO (with respect to the PM) corrections. Thus we demonstrate that k_T -factorization approach collects already at the LO the major part of the contributions which play the role of the NLO (and even NNLO) corrections to the conventional PM. Therefore we hope that a higher order (in α_S) correction to the k_T -factorization would be rather small.

Another advantage of this approach is that a non-zero transverse momentum of $Q\bar{Q}$ -system ($p_{Tpair} = p_{1T} + p_{2T} = q_{1T} + q_{2T}$) is naturally achieved in the k_T -factorization. We have calculated the p_{Tpair} distribution and compared it with the single quark p_T spectrum. At low energies the typical values of p_{Tpair} are much lesser than heavy quark p_T in accordance with collinear approximation. However for LHC energy both spectra become close to each other indicating that the transverse momentum of second heavy quark is relatively small. The typical value of this momentum ($p_{Tpair} = k_T$ -kick) depends on the parton structure functions/densities. It increases with the initial energy (k_T -kick increases with the decreasing of the momentum fractions x, y carried by the incoming partons) and with the transverse momenta of heavy quarks, p_T . Thus one gets a possibility to describe a non-trivial azimuthal correlation without introducing a large "phenomenological" intrinsic transverse momentum of the partons.

It is necessary to note that the essential values of the parton transverse momenta q_{1T} and q_{2T} increase in our calculations with the growth of the value of p_T^{min} of detected b -quark. In the language of k_T -kick it means that the values of $\langle k_T^2 \rangle$ also increase.

A more detail study of the heavy quark correlations in the k_T -factorization approach, the role of DL factor $T(k_T^2, \mu^2)$ and the value of scale μ in T -factor will be published elsewhere.

Acknowledgements

The presented calculations were carried out in ICTP. One of us (Y.M.S) is grateful to Prof. S.Randjbar-Daemi for providing this possibility and to the staff for creating good working conditions. We are grateful to Yu.L.Dokshitzer, G.P.Korchemsky and M.N.Mangano for discussions.

This work is supported by grants NATO OTR.LG 971390 and RFBR 98-02-17629.

Figure captions

Fig. 1. Heavy quark production in hadron-hadron collision. The LO parton model corresponds to the case when $q_{1T} = q_{2T} = 0$.

Fig. 2. Low order QCD diagrams for heavy quark production in pp ($p\bar{p}$) collisions via gluon-gluon fusion (a-c).

Fig. 3 The role of T -factor, Eq. (9) in the calculation of charm (solid curve) and beauty (dashed curve) production with $p_T = 20$ GeV/c at $\sqrt{s} = 14$ TeV.

Fig. 4. The total cross sections for charm and beauty hadroproduction in the k_T -factorization approach with unintegrated gluon distribution $f_g(x, q_T, \mu)$ given by Eq. (10), for μ^2 values in Eq. (9) equal to \hat{s} (solid curves), and $\hat{s}/4$ (dash-dotted curves), and in the LO parton model (dashed curves).

Fig. 5. p_T -distributions of c -quarks (a) and b -quarks (b) produced at different energies. Dashed curves are the results of the LO parton model. Solid curves are calculated with unintegrated gluon distribution $f_g(x, q_T, \mu)$ given by Eq. (10), for μ^2 values in Eq. (9) equal to \hat{s} and dash-dotted curves are calculated for $\mu^2 = \hat{s}/4$.

Fig. 6. Rapidity distributions of c -quarks (a) and b -quarks (b) produced at different energies. Dashed curves are the results of the LO parton model. Solid curves are calculated with the unintegrated gluon distribution $f_g(x, q_T, \mu)$ given by Eqs. (10), for μ^2 values in Eq. (9) equal to \hat{s} and dash-dotted curves are calculated for $\mu^2 = \hat{s}/4$.

Fig. 7. The distributions of the total transverse momentum p_{pair} for c -quarks (a) and b -quarks (b) produced at different energies (solid curves), calculated with the unintegrated gluon distribution $f_g(x, q_T, \mu)$ given by Eq. (10) and (10), for μ^2 values in Eq. (9) equal to \hat{s} . Dashed curves show the one-particle (single) p_T -distributions with the same μ^2 taken from Fig. 5. Dash-dotted and dotted curves are the same calculations for pair and single production at $\sqrt{s} = 14$ TeV with $\mu^2 = \hat{s}/4$.

Fig. 8. The calculated distributions of the rapidity difference between two c -quarks (a) or b -quarks (b) produced at different energies in the k_T factorisation approach, calculated with unintegrated gluon distribution $f_g(x, q_T, \mu)$ given by Eq. (10), for μ^2 values in Eq. (9) equal to \hat{s} (solid curves) and $\mu^2 = \hat{s}/4$ (dash-dotted curves). Dashed curves show the LO PM predictions.

Fig. 9. The calculated azimuthal correlations of charm (a) and beauty (b) pair production for $\mu^2 = \hat{s}$ (solid curves) and $\mu^2 = \hat{s}/4$ (dash-dotted curves) at the energies equal to $\sqrt{s} = 14$ TeV, 1.8 TeV, 630 GeV and 39 GeV (the latter one only for charm production).

References

- [1] P.Nason, S.Dawson and R.K.Ellis. Nucl.Phys. B303 (1988) 607.
- [2] G.Altarelli et al. Nucl.Phys. B308 (1988) 724.
- [3] P.Nason, S.Dawson and R.K.Ellis. Nucl.Phys. B327 (1989) 49.
- [4] W.Beenakker, H.Kuijf, W.L.Van Neerven and J.Smith. Phys.Rev. D40 (1989) 54.
- [5] W.Beenakker, W.L.Van Neerven, R.Meng, G.A.Schuler and J.Smith. Nucl.Phys. B351 (1991) 507.
- [6] M.N.Mangano, P.Nason and G.Ridolfi. Nucl. Phys. B373 (1992) 295.
- [7] S.Frixione, M.N.Mangano, P.Nason and G.Ridolfi. Preprint CERN-TH/97-16 (1997); hep-ph/9702287.
- [8] Yu.M.Shabelski. Talk, given at HERA Monte Carlo Workshop, 27-30 April 1998, DESY, Hamburg; hep-ph/9904492.
- [9] S.Catani, M.Ciafaloni and F.Hautmann. Phys.Lett. B242 (1990) 97; Nucl.Phys. B366 (1991) 135.
- [10] J.C.Collins and R.K.Ellis. Nucl.Phys. B360 (1991) 3.
- [11] G.Marchesini and B.R.Webber. Nucl.Phys. B386 (1992) 215.
- [12] S.Catani and F.Hautmann. Phys.Lett. B315 (1993) 475; Nucl.Phys. B427 (1994) 475.
- [13] S.Camici and M.Ciafaloni. Nucl.Phys. B467 (1996) 25; Phys.Lett. B396 (1997) 406.
- [14] L.V.Gribov, E.M.Levin and M.G.Ryskin. Phys.Rep. 100 (1983) 1.
- [15] E.M.Levin and M.G.Ryskin. Phys.Rep. 189 (1990) 267.
- [16] E.M.Levin, M.G.Ryskin, Yu.M.Shabelski and A.G.Shuvaev. Sov.J.Nucl.Phys. 53 (1991) 657.
- [17] E.M.Levin, M.G.Ryskin, Yu.M.Shabelski and A.G.Shuvaev. Sov.J.Nucl.Phys. 54 (1991) 867.
- [18] M.G.Ryskin, Yu.M.Shabelski and A.G.Shuvaev. Z.Phys. C69 (1996) 269.
- [19] Yu.M.Shabelski and A.G.Shuvaev. Eur.Phys.J. C6 (1999) 313.
- [20] M.G.Ryskin, Yu.M.Shabelski and A.G.Shuvaev. hep-ph/9907507.
- [21] M.Gluck, E.Reya and A.Vogt. Z.Phys. C67 (1995) 433.
- [22] M.Gluck, E.Reya and A.Vogt. Eur.Phys.J C5 (1998) 461.

- [23] J.C.Collins, D.E.Soper and G.Sterman. Nucl.Phys. B308 (1988) 833.
- [24] S.Narison. Phys.Lett. B341 (1994) 73; hep-ph/9503234.
- [25] P.Ball, M.Beneke and V.M.Braun. Phys.Rev. D52 (1995) 3929.
- [26] J.Blümlein. Preprint DESY 95-121 (1995).
- [27] E.A.Kuraev, L.N.Lipatov and V.S.Fadin. Sov.Phys.JETP 45 (1977) 199.
- [28] G.Marchesini and B.R.Webber. Nucl.Phys. B310 (1988) 461.
- [29] M.A.Kimber, A.D.Martin and M.G.Ryskin. hep-ph/9911379.
- [30] Yu.L.Dokshitzer, D.I.Dyakonov and S.I.Troyan. Phys.Rep. 58 (1980) 270.
- [31] S.J.Brodsky, G.P.Lepage and P.B.Mackenzie. Phys.Rev. D28 (1983) 228.
- [32] G.P.Lepage. J.Comp.Phys. 27 (1978) 192.
- [33] J.Kwiechinski. Z.Phys. C29 (1985) 561.
- [34] M.N.Mangano, P.Nason and G.Ridolfi. Nucl. Phys. B405 (1993) 507.
- [35] Liu Wenjie, O.P.Strogova, L.Cifarelli and Yu.M.Shabelski. Phys.Atom.Nucl. 57 (1994) 844.

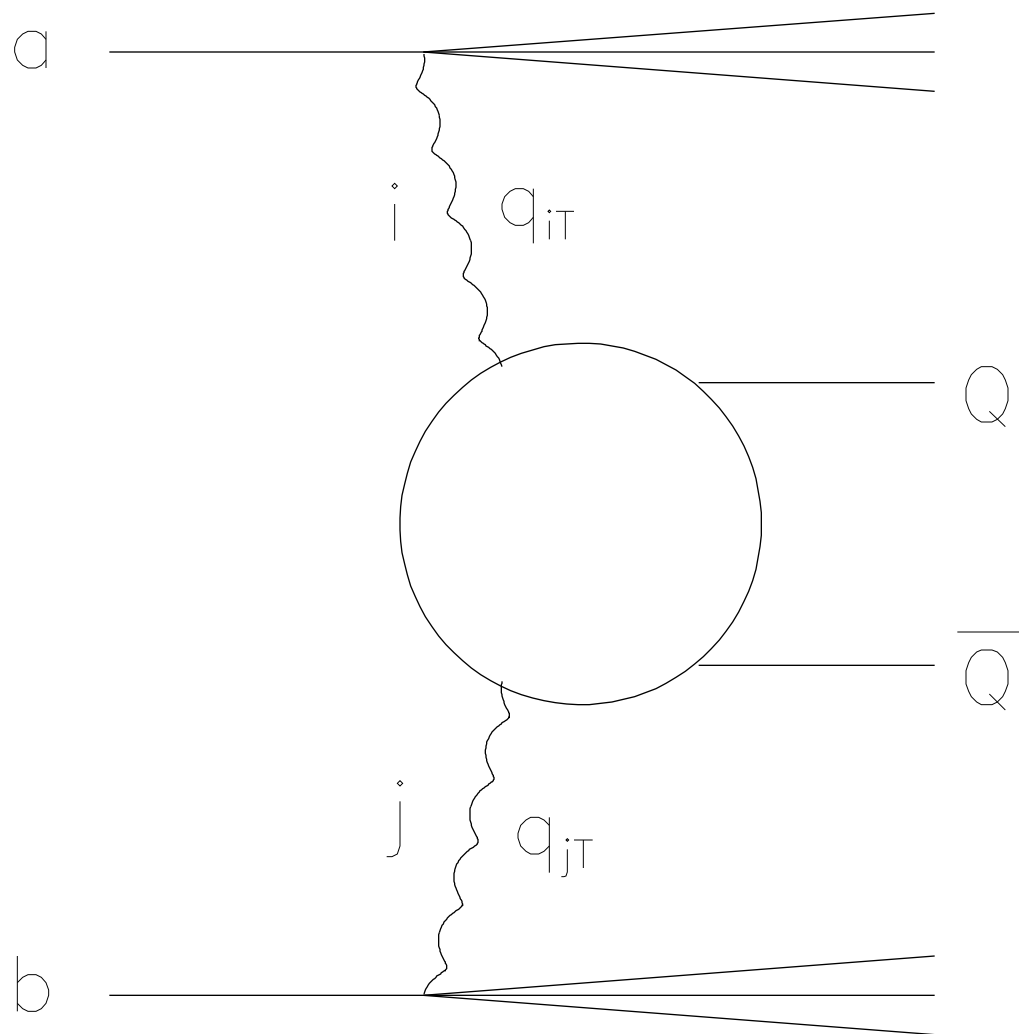


Fig. 1

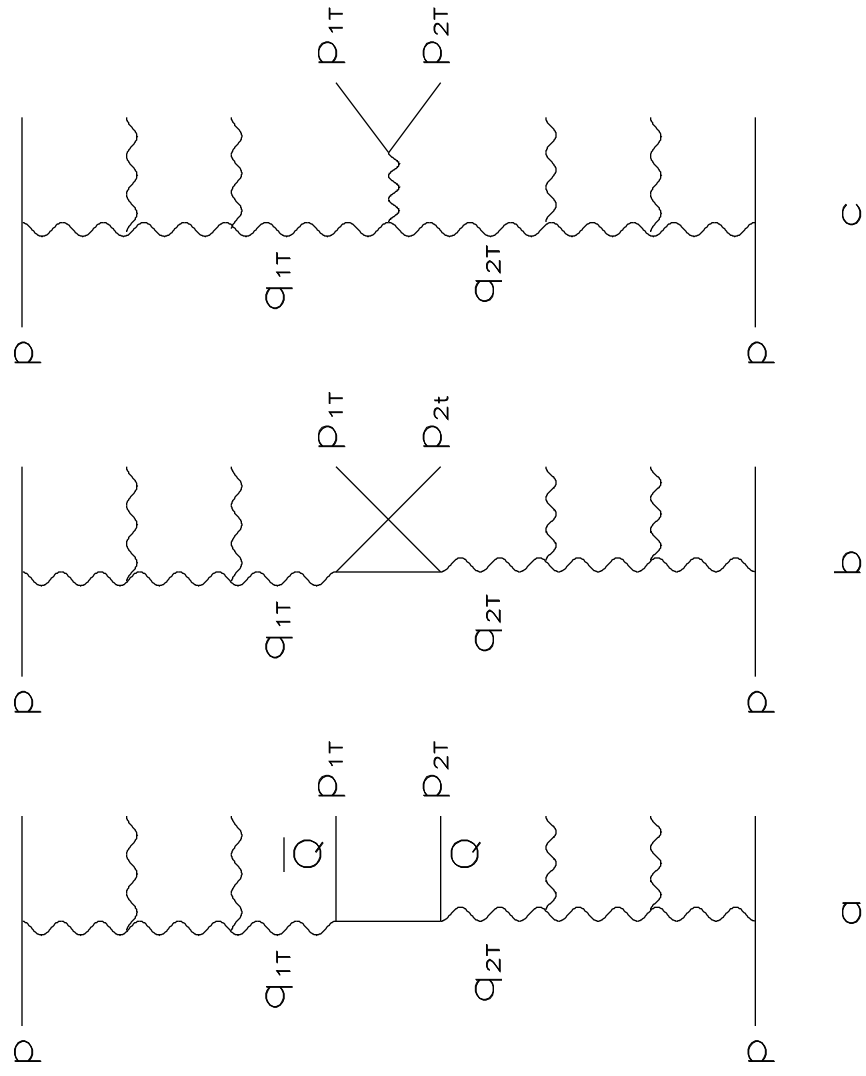


Fig. 2

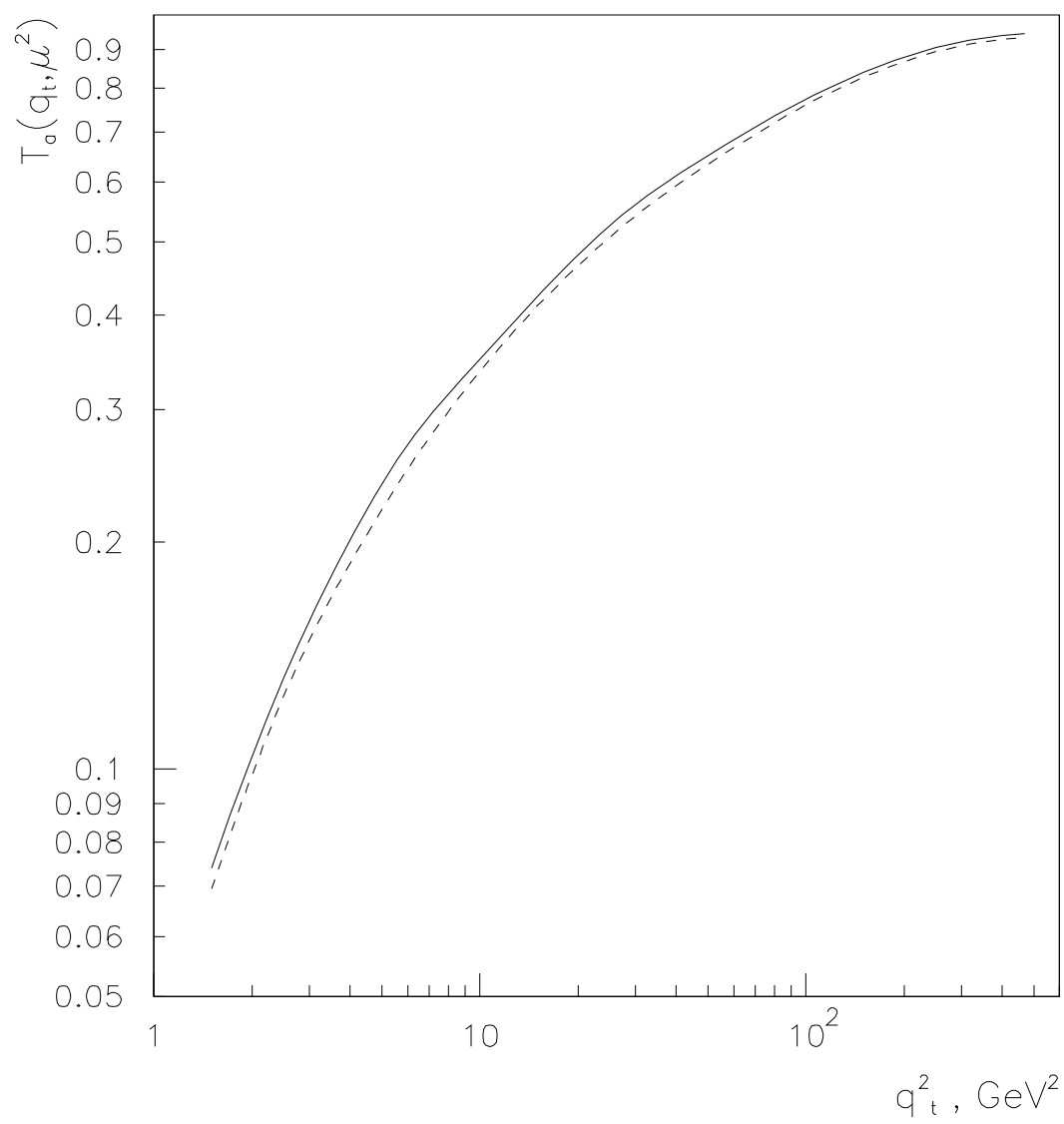


Fig. 3

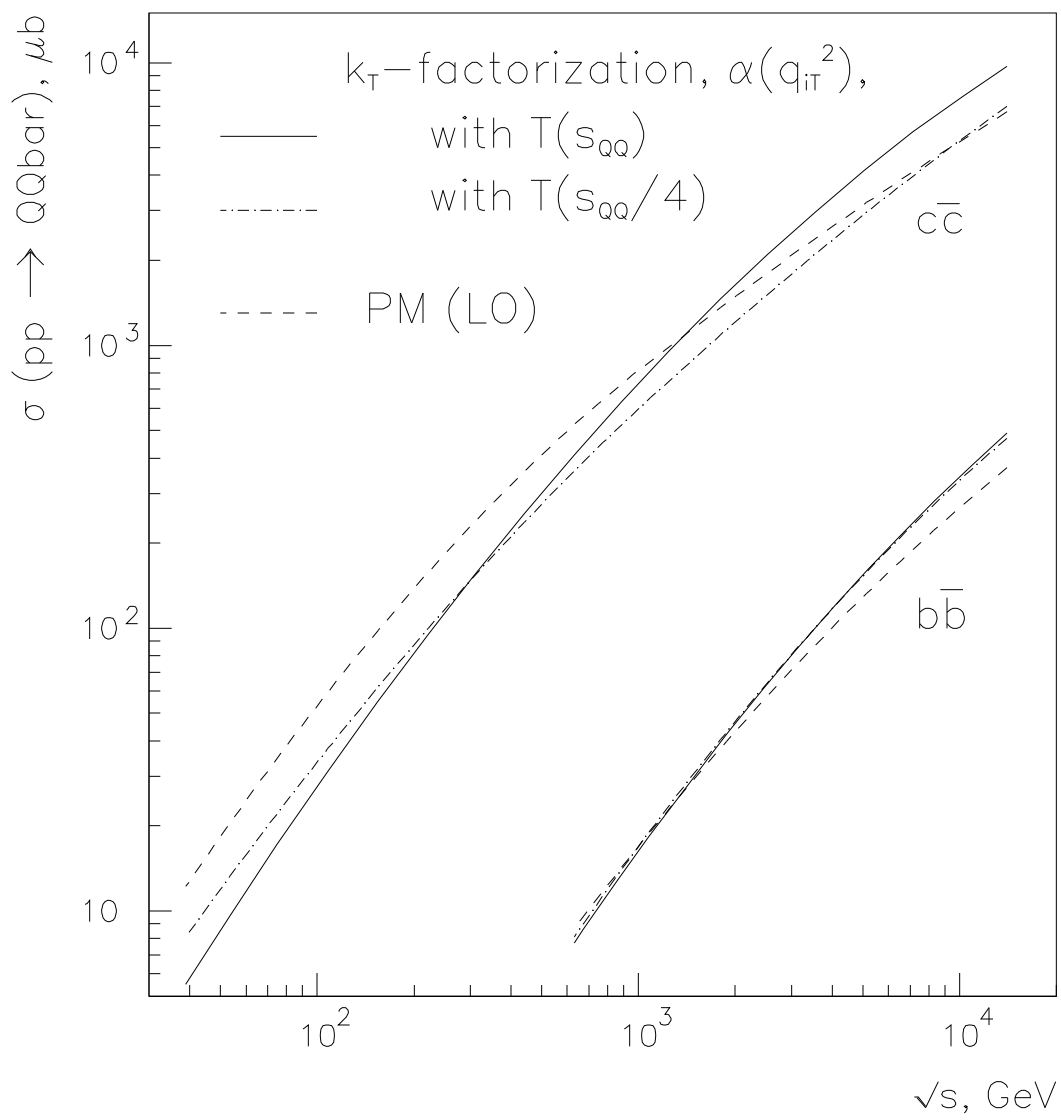


Fig. 4

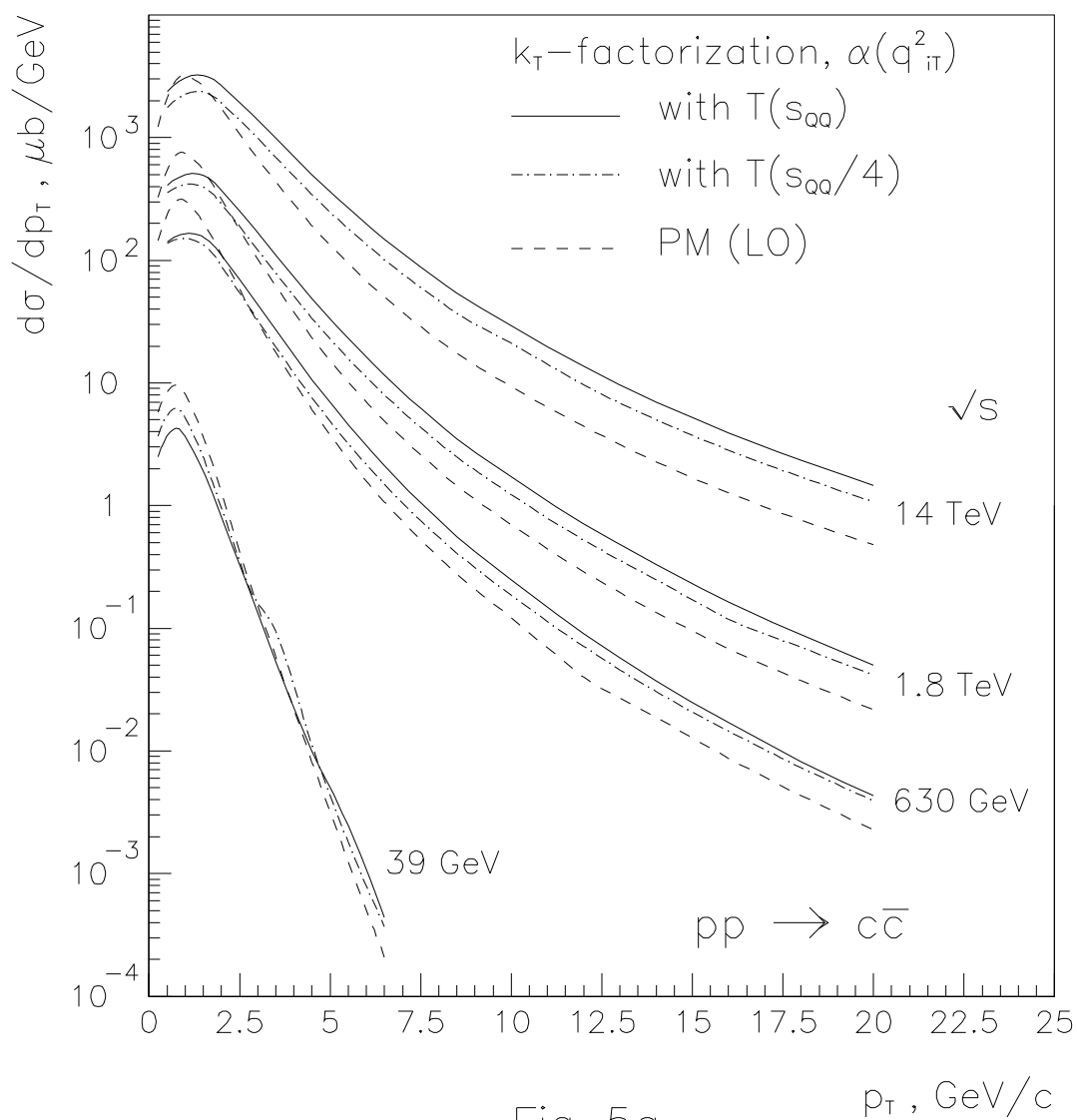


Fig. 5a

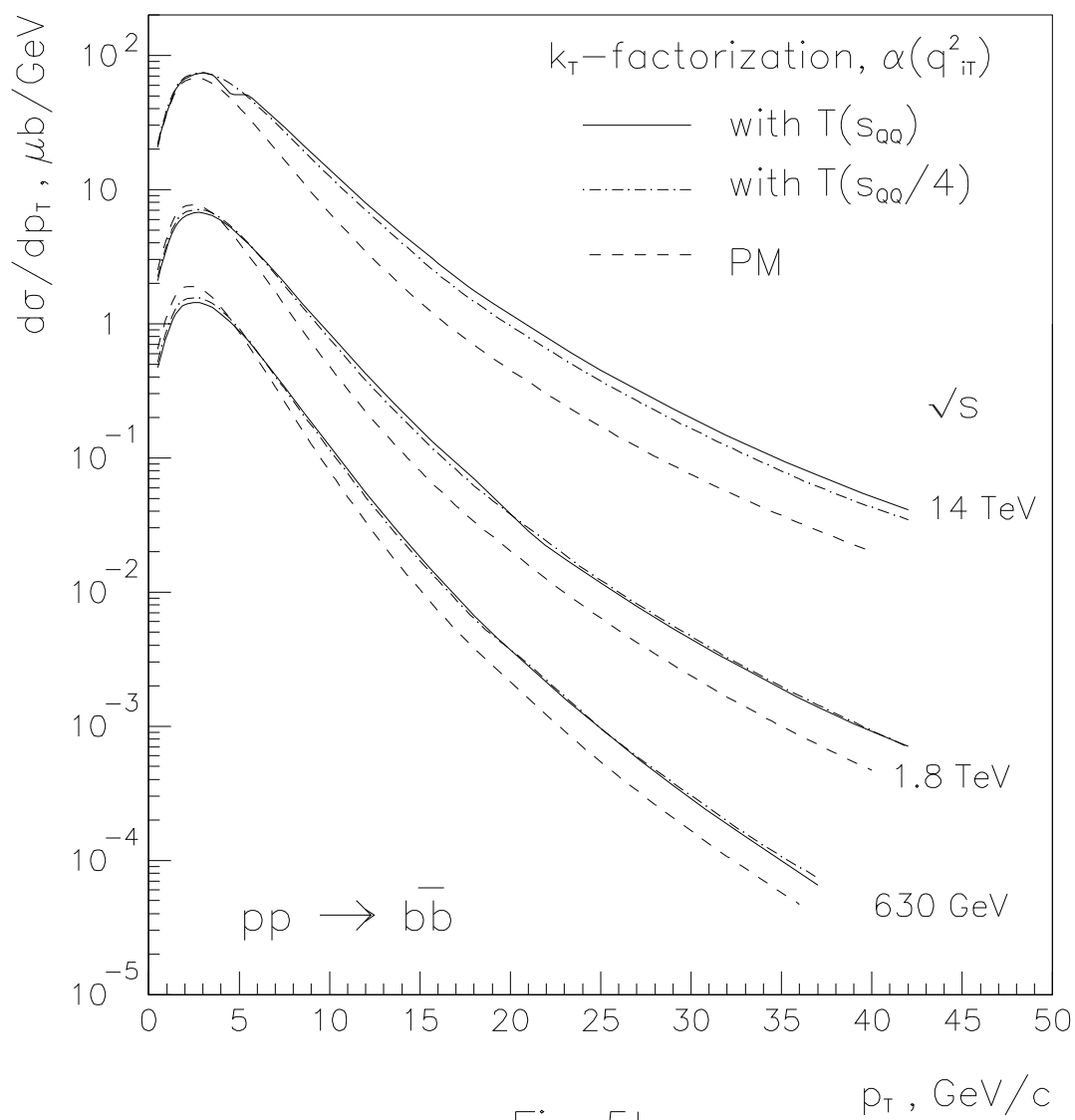


Fig. 5b

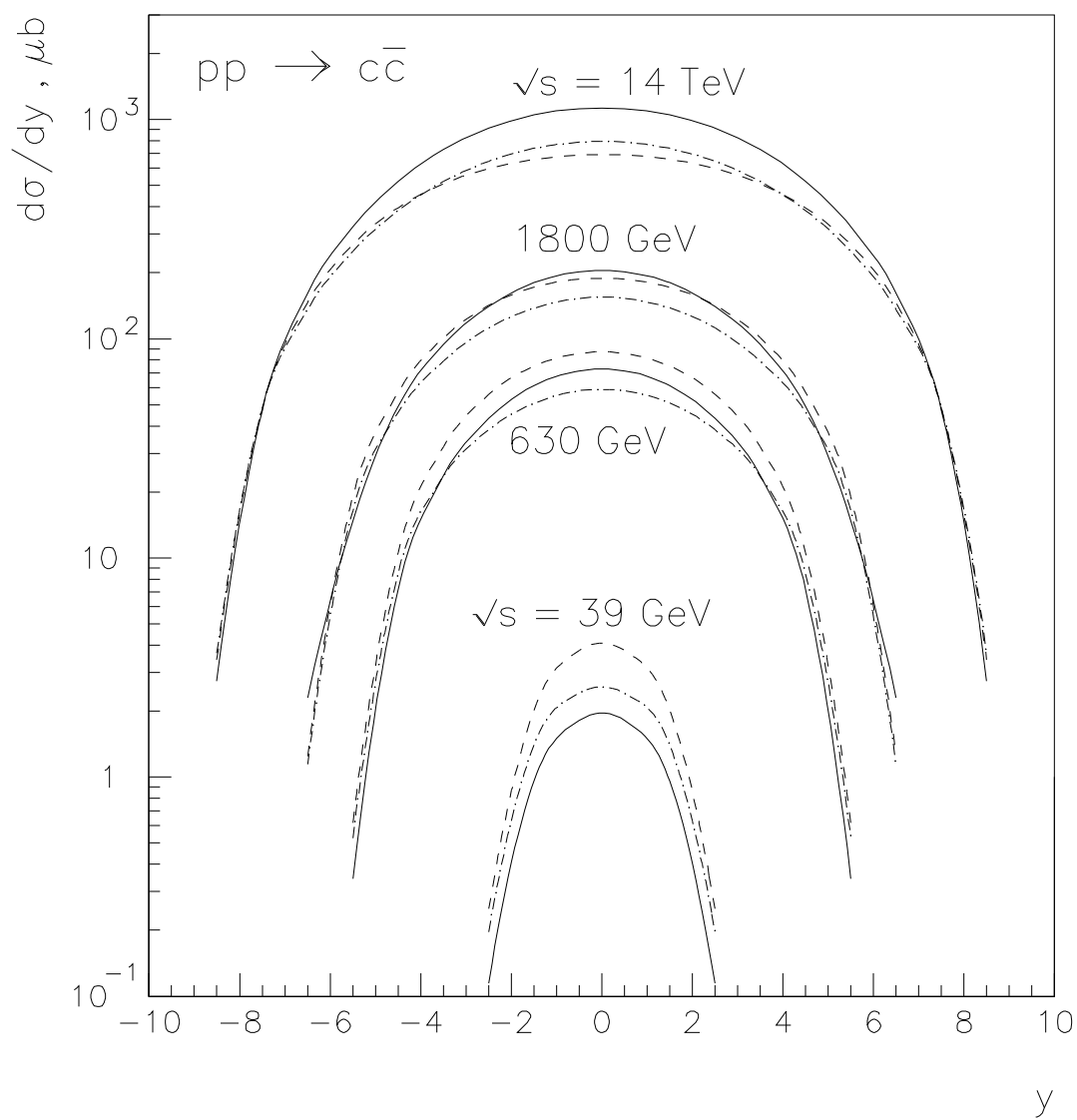


Fig. 6a

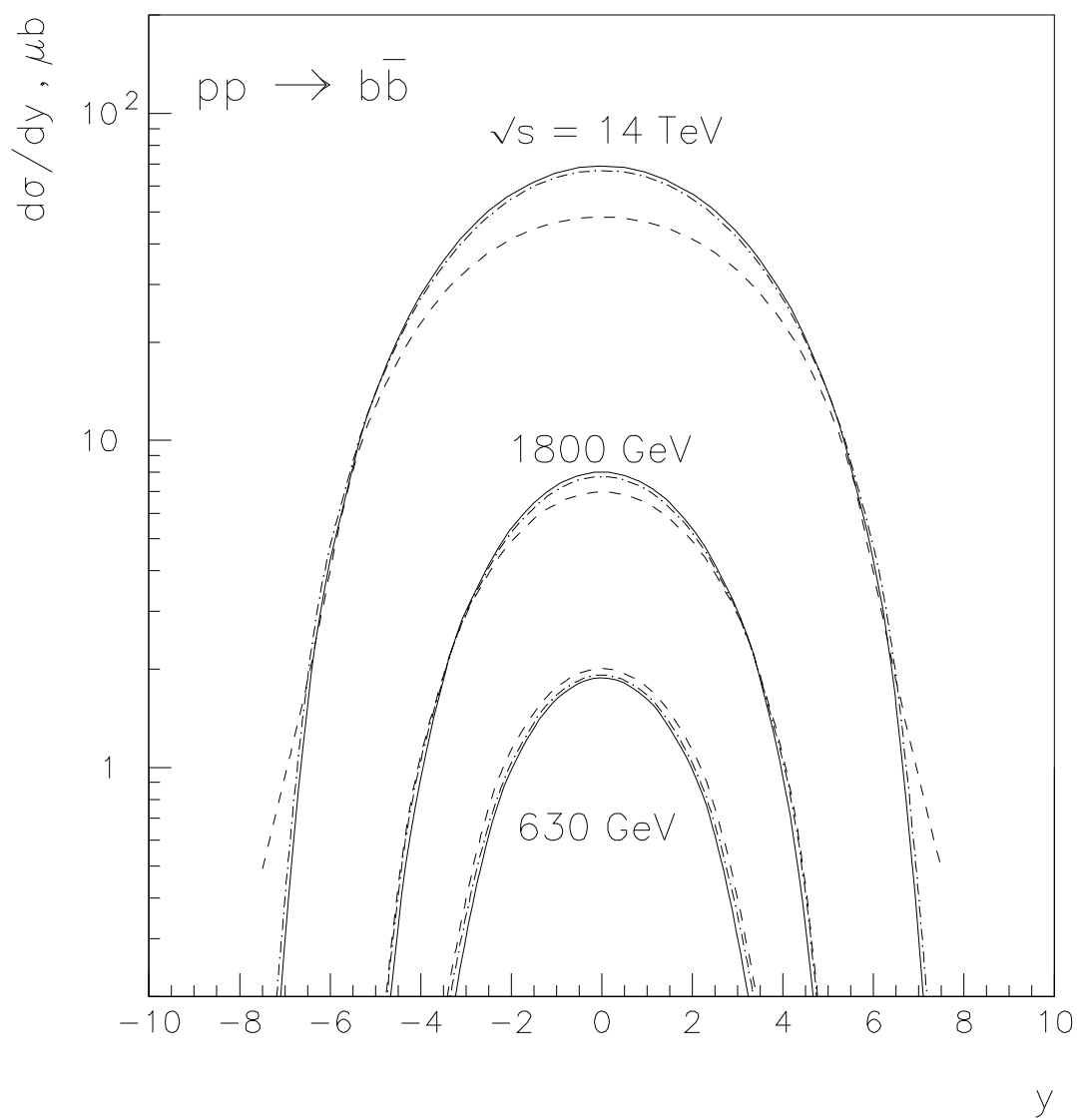


Fig. 6b

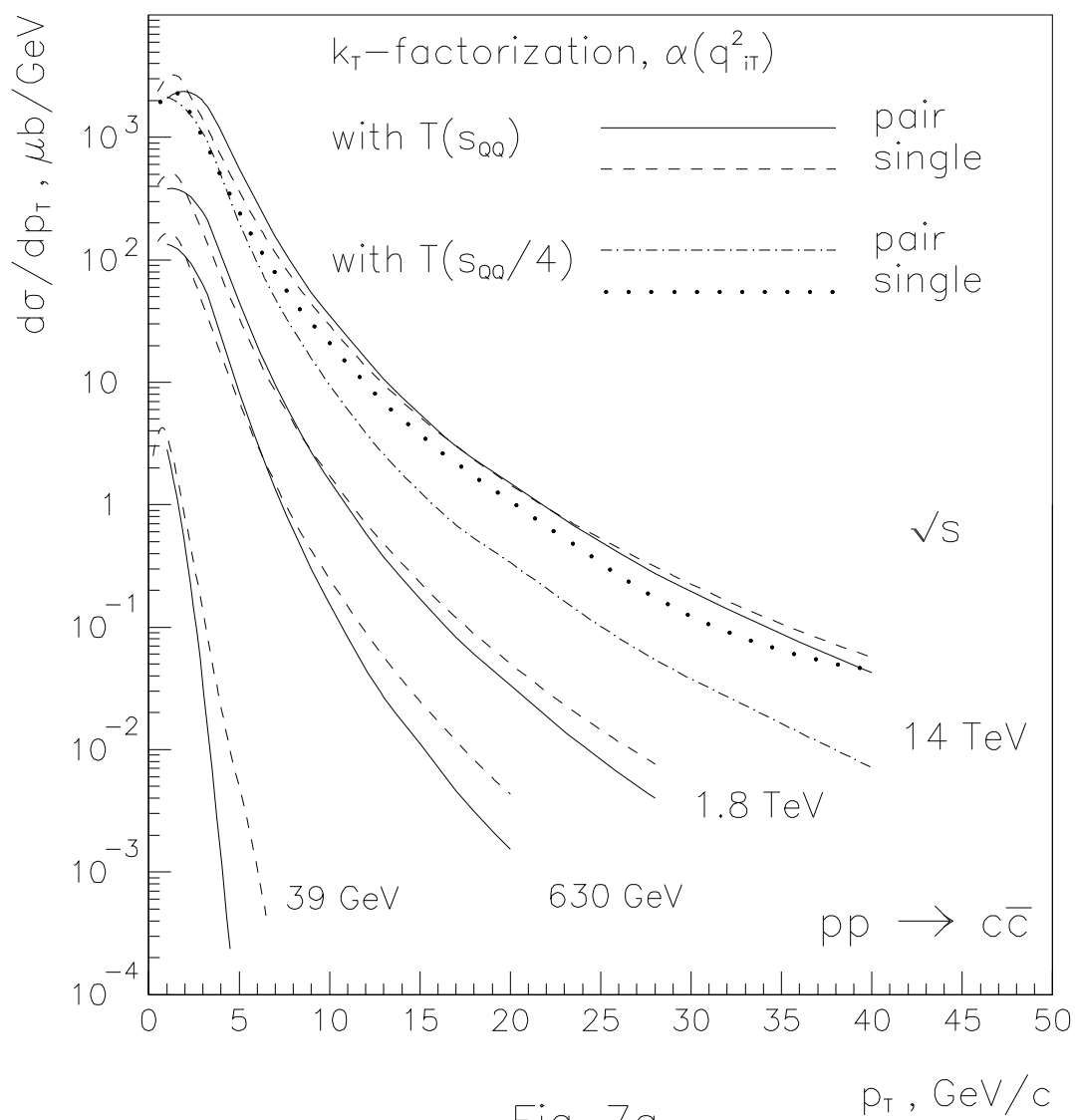


Fig. 7a

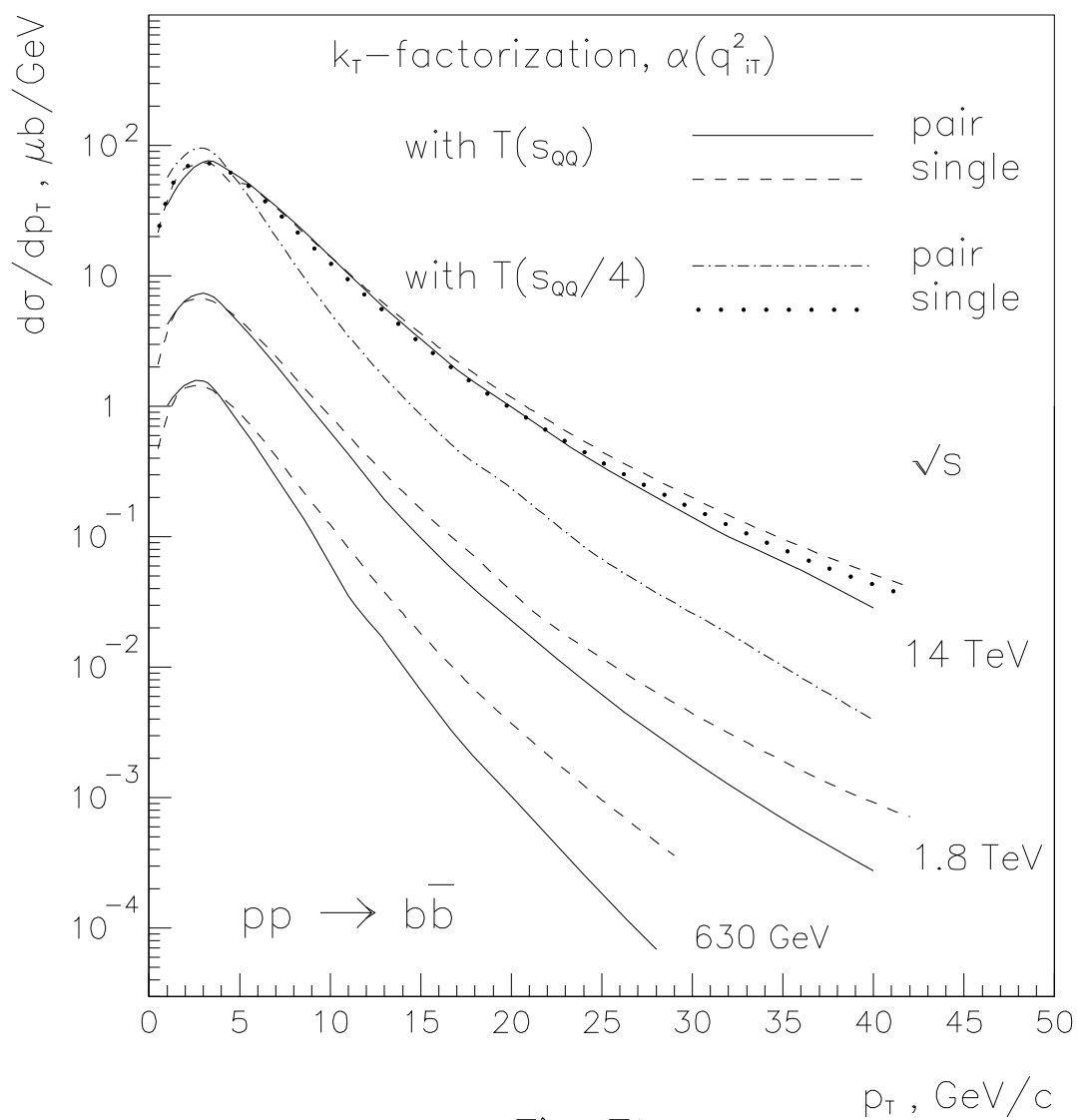


Fig. 7b

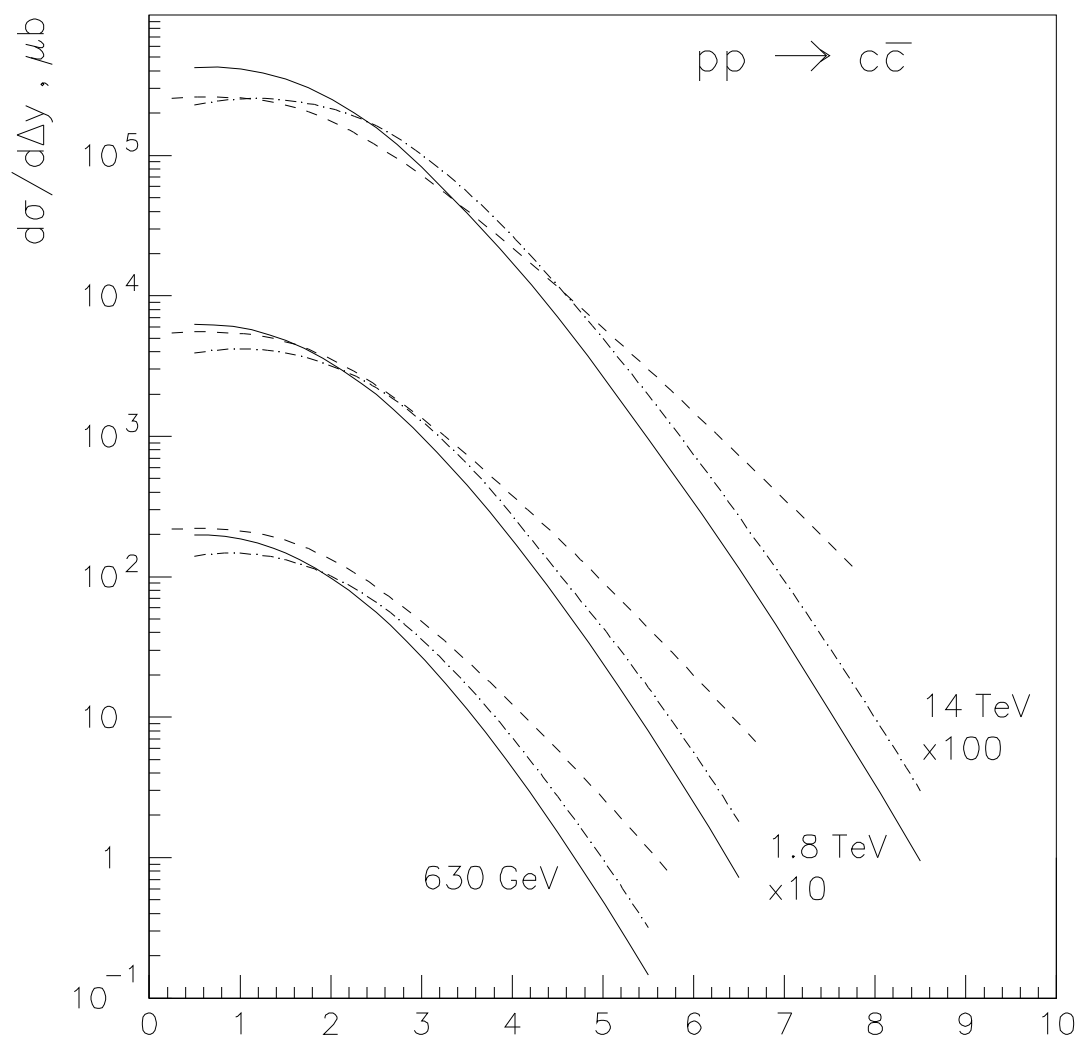


Fig. 8a

Δy

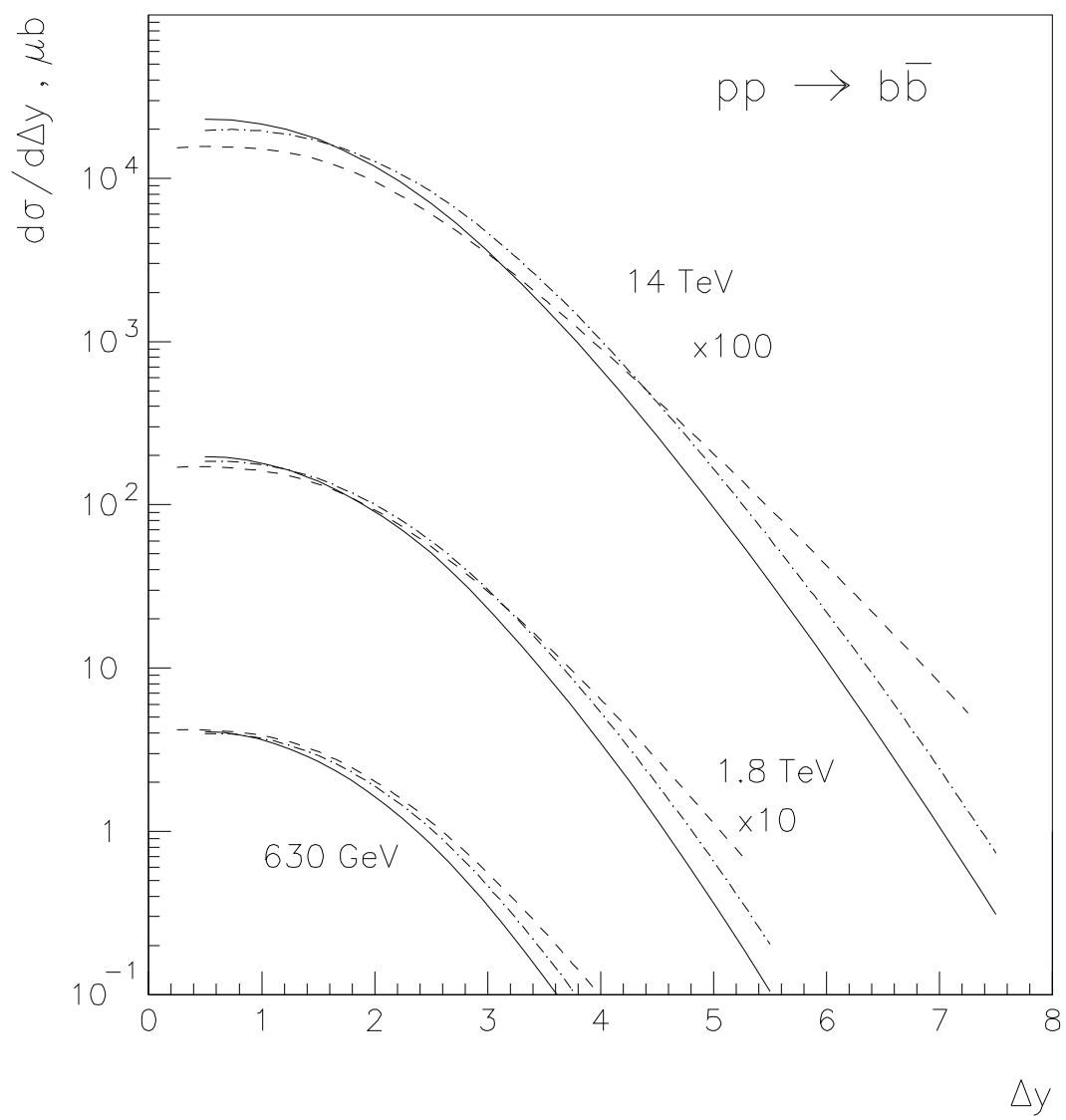


Fig. 8b

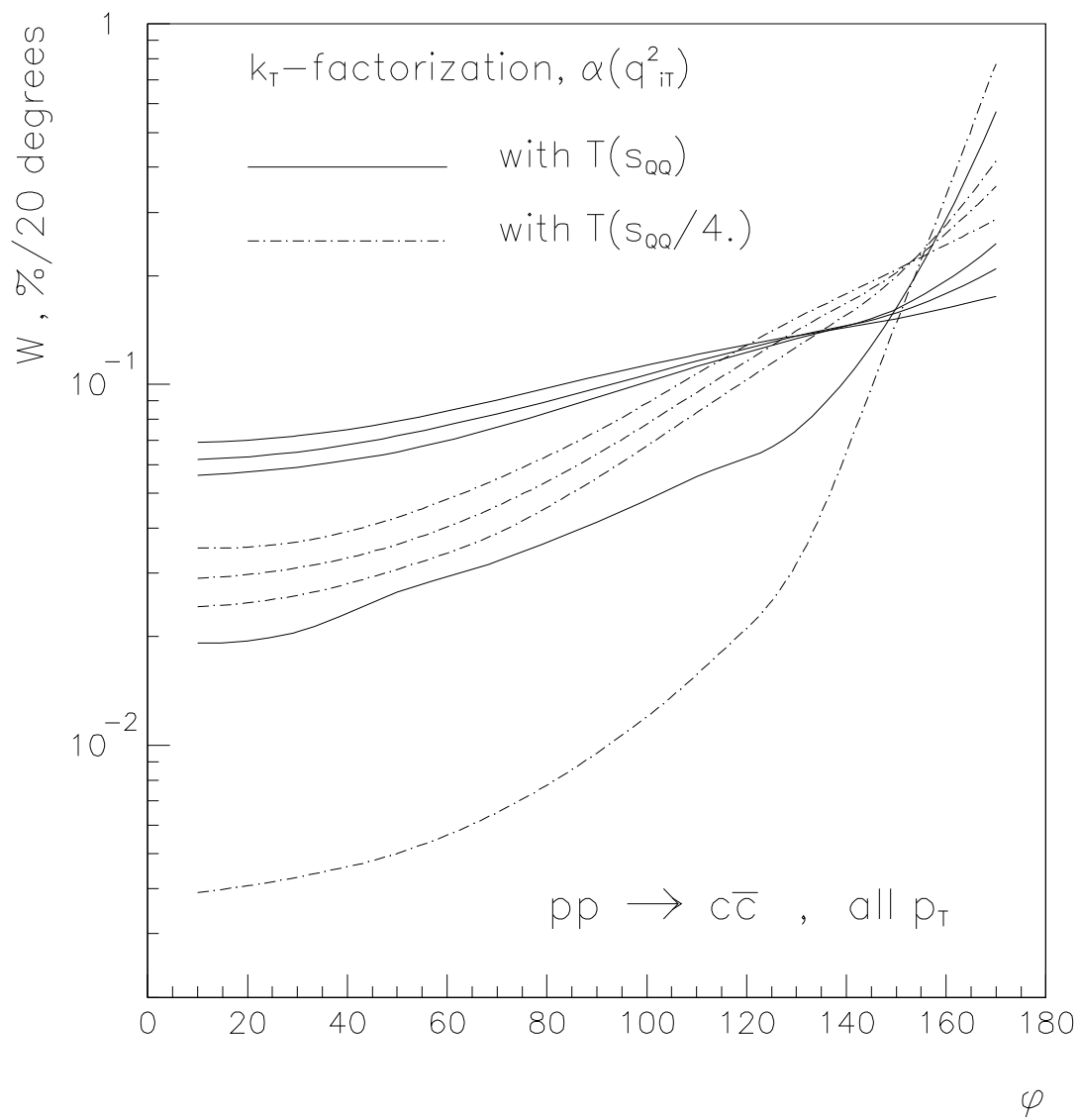


Fig. 9a

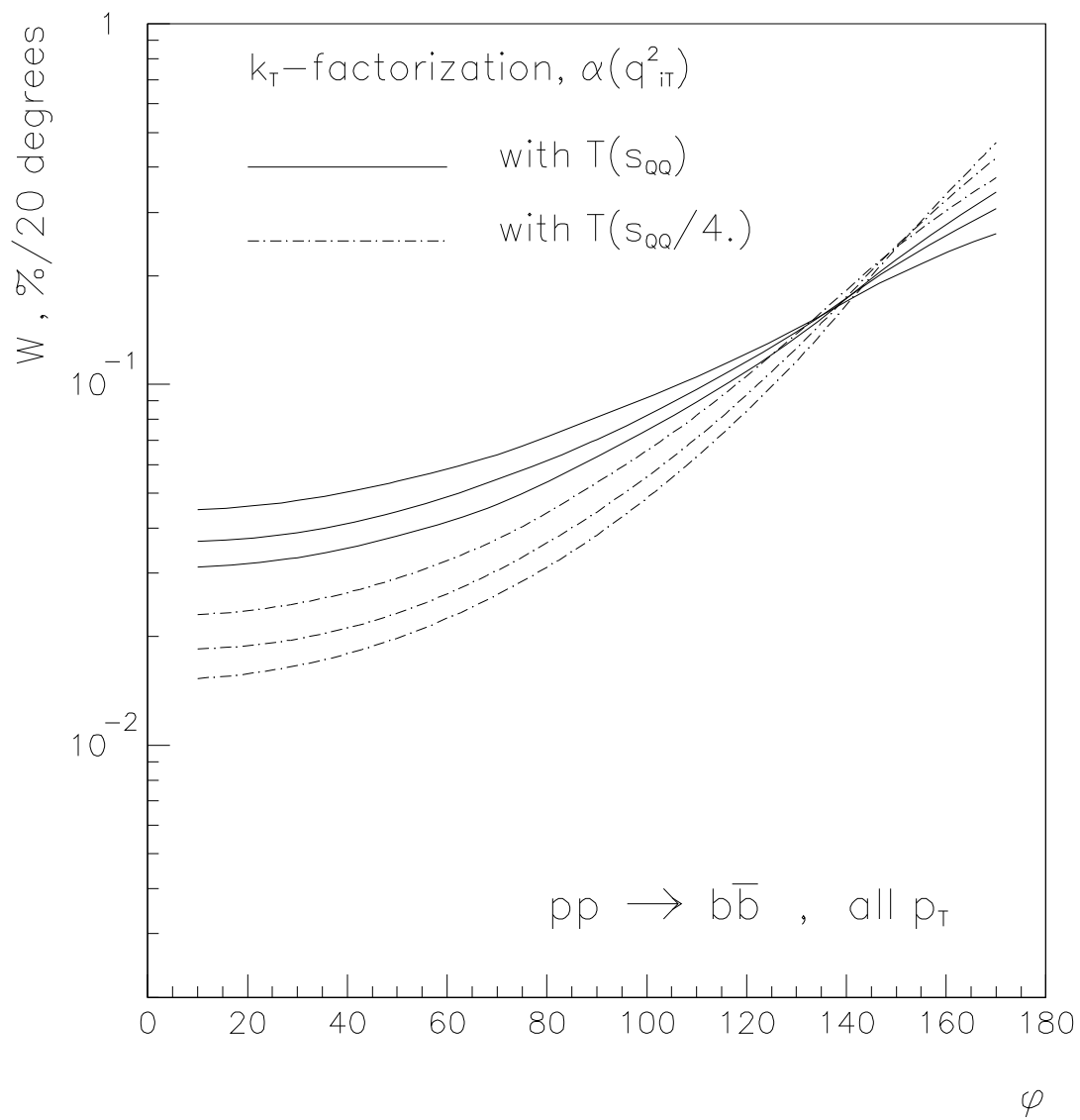


Fig. 9b